# Frequency Effect of an Oscillating Plate Immersed in a Turbulent Boundary Layer

J. J. Miau,* M. H. Chen,† and J. H. Chou‡
*National Cheng Kung University, Tainan, Taiwan, Republic of China*

**A phase-averaging technique was employed to investigate flow structures downstream of an oscillating bluff plate immersed in a turbulent boundary layer. The Reynolds number based on the maximum plate height was kept at $7.8\times10^3$. The reduced frequency of the oscillating plate was varied in a range from 0.002 to 0.013. Experimental results obtained clearly indicate that a critical reduced frequency near 0.009 can be identified, which distinguishes two types of flows of different characteristics. Under the subcritical condition (i.e., the reduced frequency less than 0.009), the flow shows a quasisteady behavior, whereas under the supercritical condition, the disturbance generated by the oscillating plate is accumulated behind the plate as the plate extends into the flow, then is released downstream as the plate retracts. A physical model concerning the flow development immediately behind the oscillating plate is proposed, which estimates that the critical reduced frequency is about 0.013, 50% higher than the experimental finding.**

## Introduction

MOTIVATED by recent interest in the control of separated flows using unsteady means,[1-6] the flow phenomena behind an oscillating plate immersed in a turbulent boundary layer are here considered. It is the authors' belief that the unsteady flow structures generated by the oscillating plate might enhance the momentum exchange between the freestream fluid and flow near the wall. Thus, boundary-layer separation originally due to an adverse pressure gradient or an abrupt change of wall geometry[7] might be suppressed by introducing this type of device.

Before implementing this concept with realistic flow conditions, it is important that one understand the physical mechanisms involved in the generation of unsteady flow structures and their evolution downstream. Owing to these concerns, the previous work[8] and the present study were performed with a flow configuration of an oscillating plate inserted into a flat-plate turbulent boundary layer. The previous experimental efforts[8] emphasized detailed flow structures generated by the oscillating plate at a chosen frequency. However, later it was found that under that experimental condition the flow actually behaved quasisteadily, as seen from the measurements of phase-averaged flow structures. As a result, two questions regarding the frequency effect of the oscillating plate were raised: 1) In what frequency range would the quasisteady interpretation of the flow be no longer valid? and 2) Was it possible to enhance momentum exchange for flow near the wall if the frequency of the oscillating plate was higher? The present paper attempts to answer these questions. As will be seen in the results obtained, a critical reduced frequency does exist in the present flow, around which a transition in flow behaviors can be identified. Above the critical frequency, the momentum exchange for flow near the wall appears more effective than that of those cases with an oscillating frequency below the critical value.

## Instrumentation and Experimental Method

A sketch of the flow configuration and coordinate system employed is shown in Fig. 1. The test section of the wind tunnel is $150\times150$ mm in cross section, in which the freestream turbulence intensity is about 0.5% for the mean velocity in a range from 2 to 20 m/s. The wind tunnel and instrumentation used in the present study are the same as those described in the authors' previous work.[8] During this experiment, the freestream velocity of the boundary layer, denoted as $U_\infty$, was fixed at 11.4 m/s and the oscillating plate was in simple harmonic motion. The height of the oscillating plate was 10 mm at its most extended position, denoted as $h_{max}$, and the plate was flush with the wall surface when it was retracted completely. Based on $h_{max}$ and $U_\infty$, the Reynolds number of the present flow was $7.8\times10^3$. The boundary-layer thickness at $X=0$, the location of the oscillating plate, was 45 mm, measured when the oscillating plate was not installed. This boundary layer was tripped by a cylindrical tube of 4.8 mm in outer diameter situated 48 cm upstream of $X=0$.

Velocity measurements were made with two sets of DANTEC 55M01 hot-wire anemometers. An X-type probe was mounted on a two-dimensional traversing mechanism, which was controlled by a 16-bit personal computer.

Most of the experimental results presented in this study were obtained through a phase-averaging technique. The phase reference was acquired from the output of a photoelectrical sensor monitoring the oscillating motion of the plate. The phase zero was denoted as the instant when the plate reached the lowest position, the position flush with the wall surface. The sampling scheme was designed in such a way that the hot-wire signal of every 2.3 cycles was taken as a sample. A collection of 100 samples obtained at the same measured position were ensemble-averaged to reveal the flow pattern.

## Dimensional Analysis

Parameters of the present flow include the plate oscillating frequency $f$, the maximum plate height $h_{max}$, the boundary-

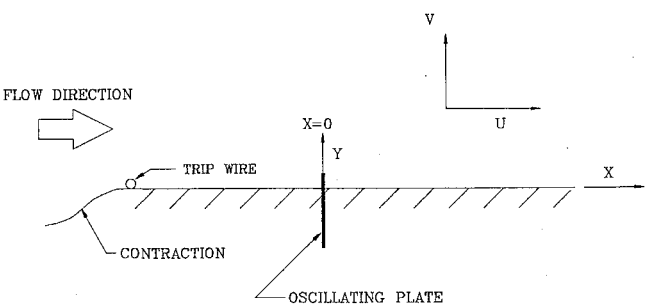


**Fig. 1 Coordinate system.**

Received Oct. 2, 1989; revision received July 1, 1990; accepted for publication Aug. 1, 1990. 

*Associate Professor, Institute of Aeronautics and Astronautics.
†Gradute Student, Institute of Aeronautics and Astronautics.
‡Professor, Department of Engineering Sciences.

layer thickness at $X=0$ without installation of the plate $\delta_{X=0}$, and the kinematic viscosity of the fluid $\nu$. After dimensional analysis, the nondimensional parameters sorted out are the Reynolds number based on $h_{max}$ and $U_\infty$, denoted as $Re = U_\infty h_{max}/\nu$, the reduced frequency denoted as $fr = fh_{max}/U_\infty$, and the ratio of $\delta_{X=0}$ and $h_{max}$, denoted as $\sigma = \delta_{X=0}/h_{max}$. In this study, although the Reynolds number $Re$ is fixed, varying $fr$ and $\sigma$ is considered.

## Undisturbed Turbulent Boundary Layer

The velocity profiles obtained in the turbulent boundary layer at $X=0$ without installation of the oscillating plate are shown in Fig. 2, in terms of the inner variables $U^+$ and $Y^+$. Here $U^+ = U/u^*$ and $Y^+ = Yu^*/\nu$, where $U$ is the local mean streamwise velocity and $u^*$ the friction velocity.[9] The straight lines in this figure come from the empirical formula for a velocity profile in the logarithmic region of a flat-plate turbulent boundary layer.[9] That is,

$$U^+ = \frac{1}{K} \ell n Y^+ + C \tag{1}$$

We employ the values of $K$ and $C$ suggested by Coles in Ref. 9 as 0.41 and 5.0, respectively. From these curves, the buffer zone, logarithmic regions, and wake region can be identified. Thus, the turbulent boundary layer is well developed at $X=0$ in the absence of the pressure gradient.

## Result and Discussion

### Phase-Average Flow Structures

Velocity measurements were made for $f=2$, 5, 8, 10, 12, and 15 Hz, respectively, in a streamwise region of $X=0$ to 71 cm. The reduced frequencies $fr$ range from 0.002 to 0.013.

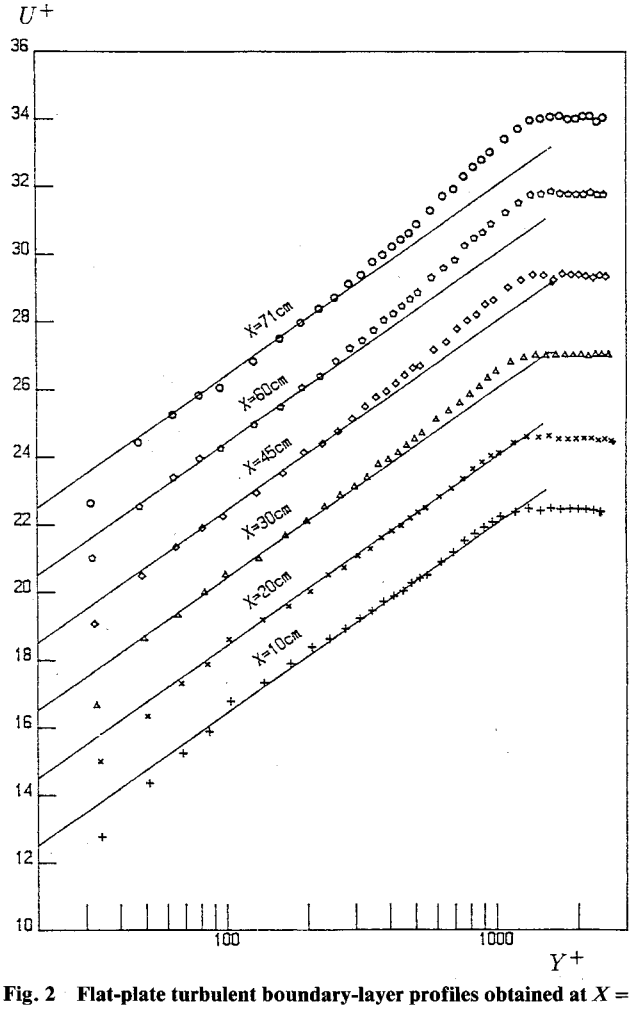


**Fig. 2 Flat-plate turbulent boundary-layer profiles obtained at $X=0$ expressed in inner variables on semilog scales.**

According to our experiences with the present flow, the unsteady flow generated by the oscillating plate took a streamwise distance of about $15$–$20h_{max}$ to develop into a well-organized form.[8] Upstream of the location $X=15h_{max}$, flow near the wall may reverse its direction for a certain period of time during each oscillation cycle of the plate. This would cause some ambiguity in interpreting the hot-wire data obtained. As a result, $X=15h_{max}$ was chosen to be the monitoring location for examining the flow characteristics under different $f$ conditions.

The ensemble-averaged two-dimensional velocity vector diagrams for $f=5$ and 15 Hz obtained at $X=15h_{max}$ are shown in Fig. 3. The plot of $f=15$ Hz is observed from a coordinate system moving with a speed of 10.7 m/s, corresponding to the mean streamwise velocity of the core of the vortical structure seen in the plot, and the plot of $f=15$ Hz refers to a coordinate system moving with a speed of 8.3 m/s, corresponding to the mean streamwise velocity of the core of the vortical structure situated closer to the wall. Note that flow is assumed to convect from right to left, to comply with the common belief that the earlier passed fluid is situated downstream. As seen in Fig. 3a for $f=5$ Hz, only one vortical structure is formed within one oscillation period of the plate, while two vortical structures are identified in the velocity vector diagrams for the case with $f=15$ Hz (see Fig. 3b). As known from our previous investigation,[8] when $f=5$ Hz, the vortical structure revealed in the plot is actually embedded in the shear layer shed from the tip of the oscillating plate, which is flapping up and down in response to the oscillating motion of the plate. For $f=15$ Hz, the vortical structures seen correspond to a situation in which the shear layer rolls up behind the oscillating plate (see also the visualizations given in Fig. 7a). The vortical structure situated above the low-speed region contains the major portion of vorticity in the shear layer, where the other structure following behind corresponds to the remaining vorticity held behind the plate that is released at a later time in the course of the plate retracting toward the wall.

The development of the unsteady shear layer behind the oscillating plate can be further examined in Fig. 4, which

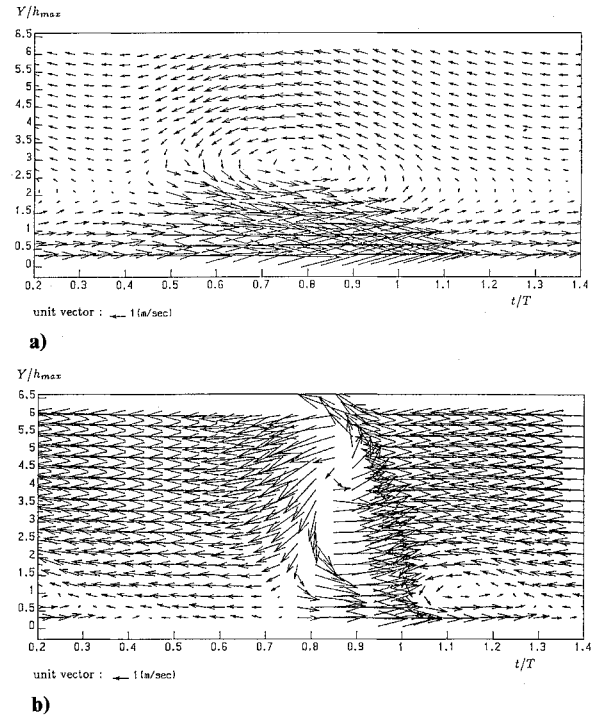


**Fig. 3 Ensemble-averged two-dimensional velocity vector diagrams obtained at $X=15h_{max}$ for: a) $f=5$ Hz and the coordinate system convecting with a speed of 10.7 m/s, and b) $f=15$ Hz and the coordinate system convecting with a speed of 8.3 m/s.**

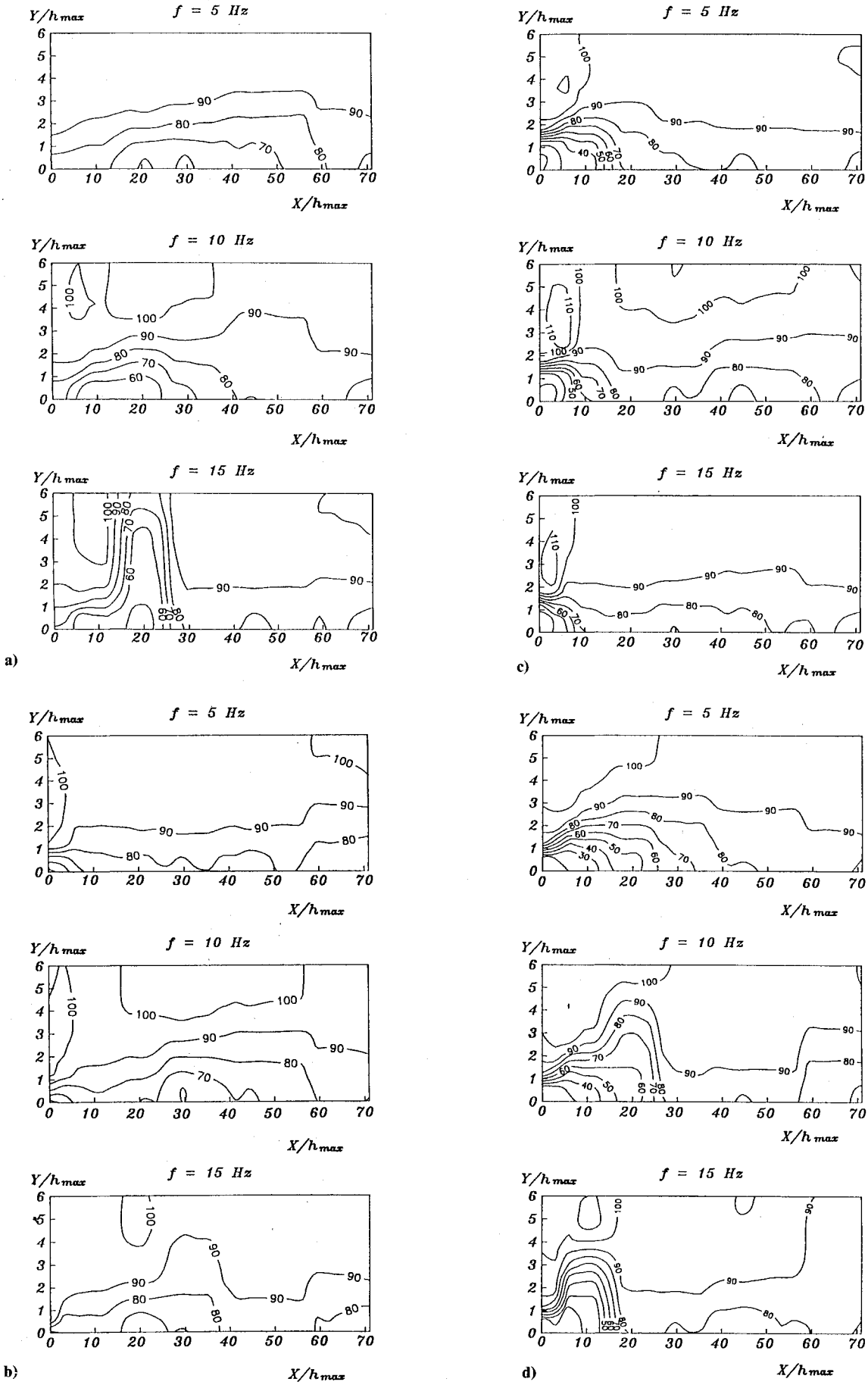


**Fig. 4 Comparison of the phase-averaged velocity contours for the cases of $f = 5$, 10, and 15 Hz. Time instants chosen for the plots are: a) $t/T = 0$, b) $t/T = \frac{1}{4}$, c) $t/T = \frac{1}{2}$, and d) $t/T = \frac{3}{4}$.**

shows the spatial distributions of the phase-averaged streamwise velocity $\langle u \rangle / U_\infty$ in the region of $X = 0$ to $71 h_{max}$. The $\langle u \rangle$ denotes the phase-averaged streamwise velocity. This figure presents a time sequence of the equi-velocity contour plots for $f = 5$, 10, and 15 Hz at $t/T = 0$, ¼, ½, and ¾, respectively. Globally speaking, these diagrams indicate that for all three $f$ cases, the evolution processes of the shear layers downstream of the oscillating plate appear similar. However, a major difference noted is that at higher frequencies, the low-speed fluid accumulated behind the oscillating plate is confined to a narrower streamwise region. This low-speed fluid region will not convect downstream until the plate retracts from the most extended position. By comparing a series of plots for different $f$, this accumulation process is noted to be the major characteristic of the unsteady flow at $f$ greater than 10 Hz. Dimensional analysis further shows that the viscous diffusion effect should not play a significant role in the phenomenon. A simple estimation of the length scale associated with the viscous diffusion effect shows that the length scale is at least an order of magnitude smaller than the characteristic size of the flow structure. Thus, the major mechanism is likely to be inviscid, which is suggested to be due to the interaction of the vorticity shed from the tip of the plate.[10]

### Critical Reduced Frequency

The experimental results suggest that when $f$ is increased over 10 Hz, the downwash motion induced by the unsteady flow structures is enhanced (see also Figs. 3 and 4). To further quantify this flow behavior, a flow quantity, namely, the minimum phase-averaged boundary-layer thickness reduced from the velocity measurements, is proposed for examination in this section. The minimum phase-averaged displacement thickness is measured at the instant when the downwash motion of the unsteady structure takes place at the measured location. Thus, a reasonable statement is that a smaller minimum phase-averaged boundary-layer thickness reflects a more intensified downwash motion in the flow.

Figure 5 shows the distributions of the minimum phase-averaged boundary-layer thickness against $f$, obtained at $X = 15 h_{max}$. The variations of the minimum phase-averaged displacement thickness and momentum thickness, i.e., $\langle \delta^* \rangle$ and $\langle \theta \rangle$, respectively, are shown for the cases with $\delta_{X=0}/h_{max} = 4.5$ and 2. The case with $\delta_{X=0}/h_{max} = 2$ was achieved by replacing the boundary-layer trip mentioned with a tube of 2 mm in outer diameter situated at the same streamwise location. These distributions indicate the same trend that they first increase with $f$ and reach a maximum value near $f = 10$ Hz, then decrease. Therefore, a transition in the minimum boundary-layer integral thickness distributions is evident around $f = 10$ Hz, which is consistent with our previous observation that the downwash motion is enhanced when $f$ is greater than this value. Accordingly, $f = 10$ Hz is regarded as the critical frequency for the present study. In the nondimensional form $f h_{max}/U_\infty$, it is about 0.009. In the following discussion, the flow condition corresponding to cases with $f$ greater than 10 Hz will be called supercritical, whereas the flow condition corresponding to cases with $f$ less than 10 Hz will be called subcritical.

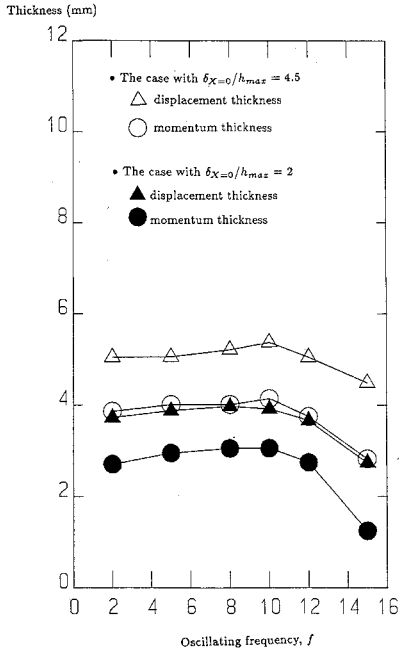


**Fig. 5 Distributions of the minimum phase-averaged boundary-layer thickness against $f$. Open symbols denote the results of the case with $\delta_{X=0}/h_{max} = 4.5$. Solid symbols denote the results of the case with $\delta_{X=0}/h_{max} = 2$.**

From this figure, it can be seen that if $\delta_{X=0}$ is reduced from 4.5 to 2 cm by changing the trip tube situated upstream, the variations of minimum $\langle \delta^* \rangle$ and $\langle \theta \rangle$ still show that the transition appears around $f = 10$ Hz. This comparison suggests that the parameter of $\delta_{X=0}/h_{max}$ seems to have an insignificant influence on the critical frequency in the range from 2 to 4.5.

It should be pointed out that while the minimum phase-averaged boundary-layer thickness decreases with $f$ as $f$ increases over 10 Hz, the maximum phase-averaged boundary-layer thickness increases with $f$ in this range. This feature is illustrated in Fig. 6, which shows the variation patterns of the phase-averaged displacement thickness for the six $f$ cases studied. By comparing the velocity vector diagrams in Fig. 3 with the present figure, one also notices that the occurrence of the maximum thickness signifies the instant when the low-speed fluid accompanying the coherent vortical structures passes the measured location. For the cases with $f = 2$ and 5 Hz, the variations of $\langle \delta^* \rangle$ appear approximately sinusoidal in time. For the case with $f = 8$ Hz and higher, the convection of low-speed fluid takes a smaller fraction of time in one oscillation period, as reflected in the phase-averaged displacement thickness patterns. For the rest of time, the boundary layer stays relatively thin.

### Estimation of the Critical Reduced Frequency

If one considers an artificial situation in which a plate is inserted into the flow from the wall abruptly and is then held at its most extended position, a separation bubble will form and expand in the rear of the plate with respect to time, similar to Pierce's[11] observation in the case of a starting flow over a wedge. Before the bubble enlarges to its stationary size, all the

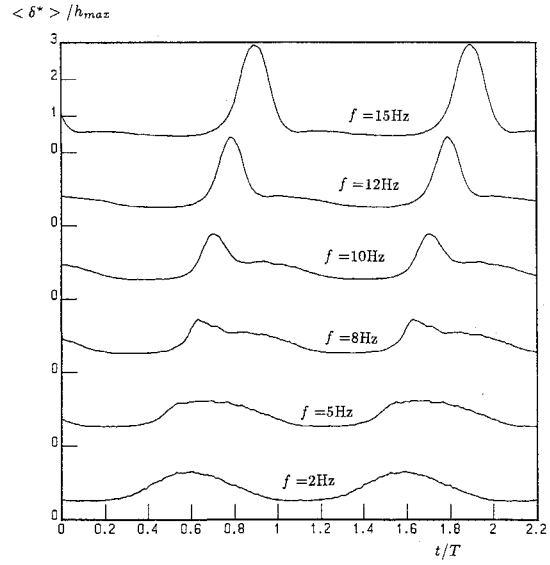


**Fig. 6 Phase-averaged displacement thickness patterns obtained at $X = 15 h_{max}$ for $f = 2$, 5, 8, 10, 12, and 15 Hz.**

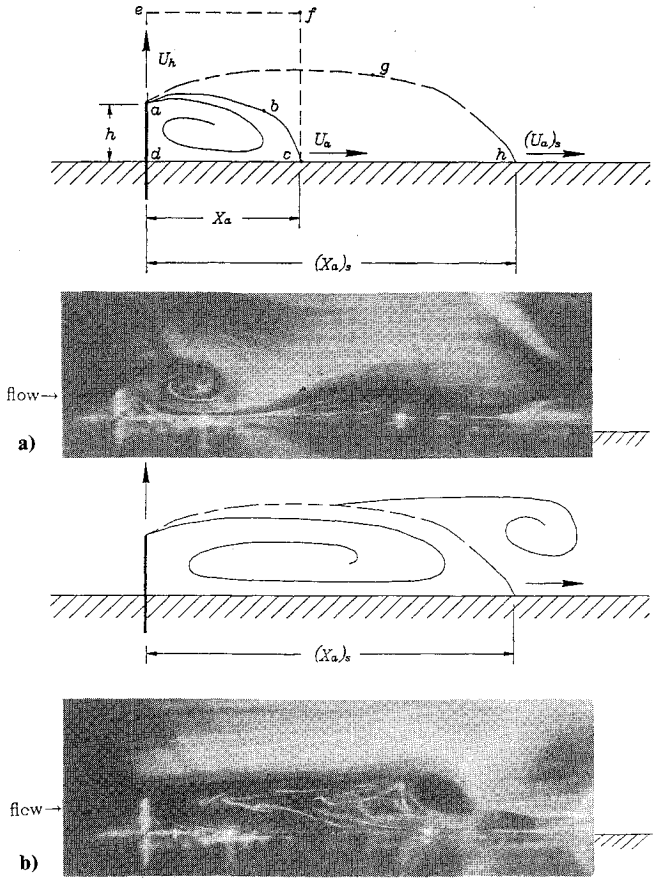


**Fig. 7 a) Sketch of flow under the supercritical condition with a smoke visualization picture taken at $K=0.05$, $t/T=0.7$ with $U_\infty=0.57$ m/s; and b) sketch of flow under the subcritical condition with a smoke visualization picture taken at $K=0.005$, $t/T=0.6$ with $U_\infty=0.57$ m/s.**

low-speed fluid tends to accumulate in the bubble. This suggests that the present unsteady flow is governed by two time scales. If the rising time of the oscillating plate is less than the time needed for the separation bubble to develop into a quasisteady size, then there would be no low-speed fluid shed away from the bubble when the plate extends upward. This is basically the situation of the supercritical case mentioned previously. On the other hand, if the rising time of the oscillating plate is longer than the time required for the separation bubble to develop into a quasisteady size, the low-speed fluid shed from the tip of the plate will overfill the separation bubble. Consequently, some of it sheds away along with time. For clarity, sketches corresponding to these two flow situations are shown in Figs. 7a and 7b, respectively. Flow visualizations relevant to these two situations are also provided. A supercritical condition fulfills the following inequality:

$$\text{vol}_D < (\text{vol}_B)_s \tag{2}$$

where $\text{vol}_D$ is the volume of the bubble developed behind the plate, and $(\text{vol}_B)_s$ is the volume of the bubble at the quasisteady state.

Let $U_a$ denote the advancing speed of the bubble front and $(U_a)_s$ be the velocity of the quasisteady state. According to Fig. 7a, the inequality of $U_a < (U_a)_s$ is held for the supercritical case. Under the critical condition, the expansion rate of the bubble is equivalent to the speed in the quasisteady state, i.e.,

$$U_a = (U_a)_s \tag{3}$$

and the low-speed fluid shed from the tip accumulates completely in the separation bubble. Note that Eq. (3) also holds for the subcritical state.

**Derivation of $(U_a)_s$**

Under the quasisteady condition, the bubble size is assumed to be similar to that in the stationary case, as indicated by the curve *agh* in Fig. 7a. Let $\gamma_h$ denote the slenderness of the stationary separation bubble behind a fixed bluff plate. Then

$$\frac{(X_a)_s}{h} = \gamma_h \simeq \text{const} \tag{4}$$

Here, $h$ denotes the plate height. So

$$(X_a)_s(t) = \gamma_h h(t) \tag{5}$$

Take the time derivative of Eq. (5)

$$(U_a)_s = \gamma_h U_h \tag{6}$$

where

$$U_h = \frac{\mathrm{d}h}{\mathrm{d}t}$$

In our case,

$$h(t) = \frac{h_{\max}}{2}(1-\cos\pi f t) \tag{7}$$

so that

$$U_h = \frac{\mathrm{d}h(t)}{\mathrm{d}t}$$

$$= \pi f h_{\max} \cdot \sin 2\pi f t \tag{8}$$

$$\Rightarrow (U_a)_s = \gamma_h \pi f h_{\max} \cdot \sin 2\pi f t \tag{9}$$

**Derivation of $U_a$**

It is assumed that 1) the flow shown in Fig. 7 is inviscid except for the region in the neighborhood of the tip of the plate where the viscous effect is necessary for vorticity generation, and 2) under the critical and supercritical conditions, all the vorticity shed is accumulated in the separation bubble *abcda*. Let $\Omega$ denote vorticity in the counterclockwise sense and $\Gamma_{abcda}$ the circulation of the path *abcda*. Then

$$\Gamma_{abcda} = \int_{abcda} (-\Omega)\,\mathbf{d}A$$

$$= \oint_{abcda} \boldsymbol{V}\cdot\mathbf{d}\boldsymbol{s} = \oint_{efcde} \boldsymbol{V}\cdot\mathbf{d}\boldsymbol{s}$$

$$= \int_{ef} \boldsymbol{V}\cdot\mathbf{d}\boldsymbol{s} + \int_{fc} \boldsymbol{V}\cdot\mathbf{d}\boldsymbol{s} + \int_{cd} \boldsymbol{V}\cdot\mathbf{d}\boldsymbol{s} + \int_{de} \boldsymbol{V}\cdot\mathbf{d}\boldsymbol{s} \tag{10}$$

where $\boldsymbol{V}$ is the velocity vector and $\boldsymbol{s}$ is the length vector tangential to the circulation path. Along path *ef*,

$$\int_{ef} \boldsymbol{V}\cdot\mathbf{d}\boldsymbol{s} \approx U_\infty X_a \tag{11}$$

Along paths *fc* and *cd*, the circulations are nearly zero, whereas along path *de*

$$\int_{de} \boldsymbol{V}\cdot\mathbf{d}\boldsymbol{s} = \int_{da} \boldsymbol{V}\cdot\mathbf{d}\boldsymbol{s} + \int_{ae} \boldsymbol{V}\cdot\mathbf{d}\boldsymbol{s} \tag{12}$$

Since the ciculation along path *ae* has a negligible contribution,

$$\int_{de} \boldsymbol{V}\cdot\mathbf{d}\boldsymbol{s} \approx \int_{da} \boldsymbol{V}\cdot\mathbf{d}\boldsymbol{s}$$

$$= U_h \cdot h(t) \tag{13}$$

From Eqs. (10), (11), and (13), we obtain

$$\Gamma_{abcda} \approx U_\infty X_a + U_h \cdot h(t) \tag{14}$$

Take the time derivative

$$\Rightarrow \dot{\Gamma}_{abcda} \approx U_\infty \dot{X}_a + \frac{\mathrm{d}}{\mathrm{d}t}\left[U_h \cdot h(t)\right]$$

$$= U_\infty U_a + \frac{\mathrm{d}}{\mathrm{d}t}\left[U_h \cdot h(t)\right] \tag{15}$$

On the other hand, the rate of vorticity accumulated in the region *abcda* is equivalent to the sum of the vorticity flux shed from the tip of the plate, denoted as $\dot{\Gamma}_s$, and the vorticity generated by the motion of the oscillating plate, denoted as $\dot{\Gamma}_p$. This is expressed as

$$\dot{\Gamma}_{abcda} \approx \dot{\Gamma}_s + \dot{\Gamma}_p \tag{16}$$

It is known that the flux of vorticity convecting in the shear layer can be expressed as[12]

$$\dot{\Gamma}_s = \tfrac{1}{2}(U_1^2 - U_2^2) \tag{17}$$

where $U_1$ and $U_2$ are the velocities of the high- and low-speed sides of the shear layer, respectively. In the present case, the shear layer is shed from the tip of the plate; therefore, it is assumed that $U_1 \approx U_\infty$ and $U_2 = 0$, so

$$\dot{\Gamma}_s = \tfrac{1}{2} U_\infty^2 \tag{18}$$

Since $\dot{\Gamma}_p$ is contributed by the motion of the oscillating plate, it is estimated as follows:

$$\Gamma_p \approx U_h \cdot h(t) \tag{19}$$

$$\Rightarrow \dot{\Gamma}_p = \frac{\mathrm{d}}{\mathrm{d}t}\left[U_h \cdot h(t)\right] \tag{20}$$

From Eqs. (16), (18), and (20),

$$\dot{\Gamma}_{abcda} \approx \frac{1}{2} U_\infty^2 + \frac{\mathrm{d}}{\mathrm{d}t}\left[U_h \cdot h(t)\right] \tag{21}$$

Equating Eqs. (15) and (21) gives

$$\Rightarrow U_\infty U_a \approx \tfrac{1}{2} U_\infty^2 \tag{22}$$

$$\Rightarrow U_a \approx \tfrac{1}{2} U_\infty \tag{23}$$

If we express $U_a$ as a fraction of $U_\infty$,

$$U_a = \gamma_U U_\infty \tag{24}$$

$$\Rightarrow \gamma_U \approx 0.5 \tag{25}$$

**Derivation of Critical Reduced Frequency**

It is seen that in Eq. (23) $U_a$ is nearly constant, whereas in Eq. (9) $(U_a)_s$ varies with time. Therefore, the criterion of the critical condition suggested by Eq. (3) is subject to modification. The present modification is based on the assumption that the critical state is reached if at any time instant in one cycle of plate oscillation, the bubble expansion rate is on the verge of being less than the quasisteady speed. The reason for this is that once the bubble expansion rate is less than the speed of the quasisteady state, the accumulation process of the low-speed fluid behind the plate will deviate from a quasisteady appearance. Therefore, this modification leads to the following expression:

$$U_a = \max\left[(U_a)_s\right] \tag{26}$$

Let $f_{cr}$ denote the critical oscillating frequency. Equation (9) shows that

$$\max\left[(U_a)\right] = \gamma_h(\pi f_{cr} h_{max}) \tag{27}$$

which occurred at the time instant $t/T = \frac{1}{4}$. Substitute Eqs. (24) and (27) into Eq. (26).

$$\gamma_U U_\infty = \gamma_h(\pi f_{cr} h_{max}) \tag{28}$$

$$\Rightarrow \frac{f_{cr} h}{U_\infty} = \frac{\gamma_U}{\pi \gamma_h}$$

$$= 0.32 \frac{\gamma_U}{\gamma_h} \tag{29}$$

According to Good and Joubert,[13] $\gamma_h \approx 10 \sim 13$ for the same flow configuration under the stationary condition. If we take $\gamma_h = 12$ and $\gamma_U = 0.5$ in Eq. (29), the critical reduced frequency is estimated to be 0.013. This value is noted to be about 50% higher than the critical reduced frequency observed in the experiments, 0.009.

In Eq. (24), the value of $\gamma_U = 0.5$ is obtained with an assumption that the vorticity convection rate of the shear layer shed from the tip of the plate is $\frac{1}{2} U_\infty^2$; see Eq. (18). Nevertheless, it should be pointed out that this value is very likely overestimated since the velocity on the high-speed side of the shear layer is not always close to the freestream velocity. If we refer to Reynolds and Carr,[4] the growth rate of the separation region behind an oscillating plate[2] and a flapping spoiler[1] can be correlated in the form

$$U_a/U_\infty = 2.44\sqrt{K} \tag{30}$$

for $0.003 < K < 0.06$, in terms of the parameters adopted in the present study. Reynolds and Carr[4] showed that the value of $U_a/U_\infty$ would not reach 0.5 until $K$ is greater than 0.6. According to Eq. (30), the value of $U_a/U_\infty$ corresponding to the critical frequency found in the present experiment, $K = 0.009$, is about 0.24.

The value of $\gamma_h = 12$ that is obtained from the case of a plate fixed in the boundary layer is likely too high if the plate is in motion in the boundary layer. The experimental results for the quasisteady case of $f = 5$ Hz indicate that when the separation bubble reaches $X = 2$, 6, and $10h$, the values of $\gamma_h$ are 7.0, 8.8, and 11.1, respectively. Consequently, if one adopts the $\gamma_U$ value of 0.24 given by Eq. (30) and an average of the $\gamma_h$ values obtained from the experiments, the resultant critical frequency of Eq. (29) would be lower than, but close to, 0.009. This check confirms the validity of Eq. (29) in the present flow phenomena.

Alternately, the critical reduced frequency can be estimated from the calculation next shown. According to the present physical model, the critical condition is characterized by a growth rate of the separation region behind an extending plate equivalent to that under the quasisteady condition. The growth rate of the separation region under the unsteady condition is given in Eq. (30), as suggested by Reynolds and Carr[4] and Francis et al.[1] On the other hand, it is realized that the growth rate under the quasisteady condition increases with $K$. According to Eq. (6), $(U_a) = \gamma_h U_h$. The time-mean value of $U_h$ is therefore estimated to be $2fh$. If $\gamma_h = 12$, then

$$(U_a/U_\infty)_s = 24K \tag{31}$$

The critical reduced frequency can be obtained by equating Eqs. (30) and (31):

$$2.44\sqrt{K} = 24K \tag{32}$$

Thus, $K \approx 0.01$, which is very close to the present experimental finding. This estimation also evidences the existence of the critical frequency.

## Concluding Remarks

It is found from experiments that a critical reduced frequency near 0.009 exists in the present flow. The unsteady flow motion is mainly governed by two time scales, one of which is the period of the oscillating motion of the plate and the other the time for vorticity accumulated in the separation region behind the oscillating plate. Under the subcritical condition, i.e., the former time scale is longer than the latter one, the flow behaves quasisteadily, whereas under the supercritical condition, the vorticity shed from the tip of the oscillating plate is mostly held in the separated bubble while the plate extends upward. This corresponds to a situation in which the shear layer shed from the tip of the oscillating plate rolls up into organized vortical structures. As the vortical structures are released downstream, the freestream fluid can be induced much closer toward the wall.

## Acknowledgment

This work was supported by the National Science Council, Republic of China, Contracts NSC 76-0401-E006-08 and NSC 77-0401-E006-38. The authors would also like to thank G. R. Chen for providing the visualizations for this paper.

## References

[1]Francis, M. S., Keesee, J. E., Lang, J. D., Sparks, G. W., Jr., and Sisson, G. E., "Aerodynamic Characteristics of an Unsteady Separated Flow," *AIAA Journal*, Vol. 17, No. 12, 1979, pp. 1332–1339.

[2]Koga, D. J., "Control of Separated Flow Fields Using Forced Unsteadiness," Ph.D. Thesis, Illinois Inst. of Technology, 1983.

[3]Nagib, H. M., Reisenthel, P. H., and Koga, D. J., "On the Dynamical Scaling of Forced Unsteady Separated Flows," AIAA Paper 85-0553, March 1985.

[4]Reynolds, W. C., and Carr, L. W., "Review of Unsteady, Driven, Separated Flows," AIAA Paper 85-527, 1985.

[5]Katz, Y., Nishri, B., and Wygnanski, I., "The Delay of Turbulent Boundary Layer Separation by Oscillatory Active Control," AIAA Paper 89-0975, 1989.

[6]Roos, F. W., and Kegelman, J. T., "Structure and Control of Flow over a Backward-Facing Step," *Forum on Unsteady Flow Separation*, edited by K. N. Ghia, American Society of Mechanical Engineers, 1987, pp. 215–223.

[7]Miau, J. J., Lee, K. C., Chen, M. H., and Chou, J. H., "Control of Separated Flow by a Two-Dimensional Oscillating Fence," *AIAA Journal* (accepted for publication).

[8]Miau, J. J., Chen, M. H., and Chou, J. H., "Flow Structure of a Vertically Oscillating Plate Immersed in a Flat-Plate Turbulent Boundary Layer," *11th Symposium on Turbulence*, Univ. of Missouri at Rolla, Rolla, MO, Oct. 17–19, 1988.

[9]White, F. M., *Viscous Fluid Flow*, McGraw-Hill, New York, 1974, Chap. 6, pp. 453–575.

[10]Rosenhead, L., "The Formation of Vortices from a Surface of Discontinuity," *Proceedings of Royal Society of London*, Series A, Vol. 134, 1931, pp. 170–192.

[11]Pierce, D., "Photographic Evidence of the Formation and Growth of Vorticity Behind Plate Accelerated from Rest in Still Air," *Journal of Fluid Mechanics*, Vol. 11, Pt. 3, 1961, pp. 460–464.

[12]Sears, W. R., "Some Recent Developments in Airfoil Theory," *Journal of the Aeronautical Sciences*, Vol. 23, No. 5, 1956, pp. 490–499.

[13]Good, M. C., and Joubert, P. N., "The Form Drag of Two-Dimensional Bluff-Plates Immersed in Turbulent Boundary Layers," *Journal of Fluid Mechanics*, Vol. 31, Pt. 3, 1968, pp. 547–582.